

## Coupled-Cluster and Configuration-Interaction Calculations for Heavy Nuclei

M. Horoi,<sup>1</sup> J. R. Gour,<sup>2</sup> M. Włoch,<sup>2</sup> M. D. LoDriguito,<sup>2</sup> B. A. Brown,<sup>3</sup> and P. Piecuch<sup>2,3</sup>

<sup>1</sup>*Department of Physics, Central Michigan University, Mount Pleasant, Michigan 48859, USA*

<sup>2</sup>*Department of Chemistry, Michigan State University, East Lansing, Michigan 48824, USA*

<sup>3</sup>*Department of Physics and Astronomy and National Superconducting Cyclotron Laboratory, Michigan State University, East Lansing, Michigan 48824, USA*

(Received 4 December 2006; published 13 March 2007)

We compare coupled-cluster (CC) and configuration-interaction (CI) results for  $^{56}\text{Ni}$  obtained in the  $pf$ -shell basis, focusing on practical CC approximations that can be applied to systems with dozens or hundreds of correlated fermions. The weight of the reference state and the strength of correlation effects are controlled by the gap between the  $f_{7/2}$  orbit and the  $f_{5/2}$ ,  $p_{3/2}$ ,  $p_{1/2}$  orbits. Independent of the gap, the CC method with 1p-1h and 2p-2h clusters and a noniterative treatment of 3p-3h clusters is as accurate as the more demanding CI approach truncated at the 4p-4h level.

DOI: [10.1103/PhysRevLett.98.112501](https://doi.org/10.1103/PhysRevLett.98.112501)

PACS numbers: 21.60.Cs, 21.60.Gx, 27.40.+z, 31.15.Dv

As computational methods in nuclear theory advance, we are able to apply microscopic methods to the understanding of the structure of heavy nuclei. One of the recent examples is the  $pf$ -shell description of  $^{56}\text{Ni}$ , where the properties of essentially all levels up to about 8 MeV, including the coexistence of low-lying spherical states with excited deformed bands, have been understood via the full configuration-interaction (CI) calculation in the  $pf$  basis [1]. The full  $pf$ -shell calculation for  $^{56}\text{Ni}$ , with an  $M$ -scheme dimension of  $\sim 10^9$ , is a huge computational effort, which has become feasible only recently. One would like to carry out analogous calculations involving orbitals near the Fermi surface for all heavier nuclei. Unfortunately, this is not possible due to the rapid increase of the dimensionality of the full CI eigenvalue problem with the system size.

An interesting, computationally cost-efficient alternative to full CI is offered by coupled-cluster (CC) theory [2,3], which sums entire classes of many-particle correlation effects, required for an accurate description of energies and wave functions, to infinite order. The CC method started in nuclear theory [2,4], but it has been mostly developed and applied in quantum chemistry [3,5,6]. It has recently been reintroduced into nuclear theory with applications to the no-core basis of light nuclei [7,8], but much less is known about the performance of modern CC approaches for heavier nuclei where they may become useful due to the prohibitive costs of full CI calculations. Truncated CI methods reduce these costs as well, but they are not as effective in describing particle correlations as the truncated CC models and, unlike CC methods, they are not size extensive.

In this Letter, we apply practical CC methods, developed in quantum chemistry to study systems with dozens or even hundreds of correlated fermions and hundreds of basis functions [9], to the valence configuration space of heavy nuclei. The specific application to  $^{56}\text{Ni}$  is ideal because the effective Hamiltonian required for nuclei in the  $^{56}\text{Ni}$  region

is well established. In addition, the CC results can be directly compared to the exact solutions obtained with full CI, and in the  $pf$  model space there are no spurious center-of-mass contaminants that complicate the applications to light nuclei. The CC approaches used in this Letter are rooted in a many-body expansion relative to a single-determinantal reference state. Thus, the semi-closed-shell structure of  $^{56}\text{Ni}$  makes it an excellent place to test practical single-reference CC methods in a region where a single-determinantal reference state may no longer dominate the wave function. Furthermore, we can “tune” the Hamiltonian to study the accuracy of CC methods as a function of the weight of the reference state.

We use the recently developed GXPF1A effective Hamiltonian [10] that was exploited in a comprehensive study of energy levels in  $^{56}\text{Ni}$  [1]. GXPF1A was derived from a microscopic calculation by Hjorth-Jensen based on renormalized  $G$ -matrix theory with the Bonn-C interaction [11], and was refined by a systematic fitting of the important linear combinations of two-body matrix elements to low-lying states in nuclei from  $A = 47$  to  $A = 66$ , including some states of  $^{56}\text{Ni}$  [10,12]. The closed-shell properties of  $^{56}\text{Ni}$  and the strength of correlation effects are tuned by varying the energies of the  $f_{5/2}$ ,  $p_{3/2}$ ,  $p_{1/2}$  orbitals relative to a fixed energy of the  $f_{7/2}$  orbit. Thus, we change the shell gap by an amount  $\Delta G$ .  $\Delta G = 0$  is the original Hamiltonian used in [1], which gives an overlap  $S_0 = |\langle \Phi_0 | \Psi_0^{\text{Full-CI}} \rangle|$  between a closed-shell ( $f_{7/2}^{16}$ ) component, defining the reference determinant  $|\Phi_0\rangle$  for CC calculations, and the full CI ground state  $|\Psi_0^{\text{Full-CI}}\rangle$  of 0.825. We move the gap up by as much as 2 MeV to produce  $S_0 = 0.949$  and down by as much as 2 MeV to reduce  $S_0$  to 0.022.

We compare the results for the CI and CC models at various levels of approximation. All energies are given relative to the reference energy  $\langle \Phi_0 | H | \Phi_0 \rangle = -203.800$  MeV. In addition to full CI that includes all

determinants up to 16p-16h excitations relative to  $|\Phi_0\rangle$ , the CI methods used in this study include CISD (CI singles and doubles), CISDT (CI singles, doubles, and triples), and CISDTQ (CI singles, doubles, triples, and quadruples), which are obtained by truncating the CI wave function expansions at 2p-2h, 3p-3h, and 4p-4h excitations, represented here by the particle-hole excitation operators  $C_2$ ,  $C_3$ , and  $C_4$ , respectively. The CI calculations for the  $\Delta G = 0$   $^{56}\text{Ni}$  model were described in Ref. [1]. The CC models include the basic CCSD (CC singles and doubles) approximation [13] and the CR-CC(2,3) and CR-CC(2,4) methods [14], which represent the improved variants of the completely renormalized (CR) CC approaches [6] used in the earlier studies of light nuclei [8]. In the CCSD approach, the cluster operator  $T$  defining the CC ground state [2,3],  $|\Psi_0\rangle = \exp(T)|\Phi_0\rangle$ , where in the exact case  $T = T_1 + T_2 + \dots + T_A$  and  $T_n$  designates the  $np$ - $nh$  component of  $T$ , is truncated at the 2p-2h clusters  $T_2$ , i.e.,  $T = T_1 + T_2$ . Since higher-order  $T_n$  clusters with  $n > 2$  may play an increasingly important role as the shell gap and overlap  $S_0$  decrease, we correct the CCSD energies for the effects of  $T_3$  and  $T_4$  clusters. In principle, this should be done with the high-order CC schemes, such as CCSDT and CCSDTQ, in which  $T = T_1 + T_2 + T_3$  and  $T = T_1 + T_2 + T_3 + T_4$ , respectively, but a direct determination of  $T_3$  and  $T_4$  through such schemes is very expensive, defeating the main advantage of CC vs CI, which is the high computational efficiency in accounting for particle correlations. This is particularly relevant for applications of CC methods to heavier nuclei, where costs of high-order CI or CC computations can be enormous.

Thus, we exploit the inexpensive ways of incorporating  $T_3$  and  $T_4$  clusters through the CR-CC(2,3) and CR-CC(2,4) approximations [14]. In these approaches, the effects of  $T_3$  [CR-CC(2,3)] or  $T_3$  and  $T_4$  [CR-CC(2,4)] are accounted for by adding noniterative *a posteriori* corrections to the CCSD energy. As shown in [14], one can calculate such corrections using the  $T_1$  and  $T_2$  clusters obtained in CCSD calculations; i.e., one does not have to consider the  $T_3$  and  $T_4$  clusters explicitly. One of the main advantages of the CR-CC(2,3) and CR-CC(2,4) approaches is their low computational cost, enabling calculations for systems with hundreds of fermions and basis functions. The most expensive computational steps in these schemes scale as  $n_o^3 n_u^4$  [CR-CC(2,3)] or  $n_o^3 n_u^4$  and  $n_o^2 n_u^5$  [CR-CC(2,4)] in the calculation of the noniterative correction due to  $T_3$  or  $T_3$  and  $T_4$ , respectively, and  $n_o^2 n_u^4$  in the CCSD part needed to generate  $T_1$  and  $T_2$  ( $n_o$  and  $n_u$  are the numbers of occupied and unoccupied states in a single-particle basis set, respectively). This is much less than the  $n_o^3 n_u^5$  and  $n_o^4 n_u^6$  iterative steps characterizing CCSDT and CCSDTQ, respectively. One of the main findings of this work is that the CR-CC(2,3) method, with its inexpensive computational steps and use of small numbers of cluster amplitudes that are  $\sim n_o n_u$  for  $T_1$  and  $\sim n_o^2 n_u^2$  for  $T_2$ , is as accurate as the relatively expensive diagonalization of the Hamiltonian using CISDTQ. CISDTQ requires the itera-

tive  $n_o^4 n_u^6$  steps and the corresponding eigenvalue problem is large due to the presence of  $\sim n_o^4 n_u^4$  determinants of the 4p-4h type in the CISDTQ wave function. We also use the extensions of CCSD, CR-CC(2,3), and CR-CC(2,4) to excited states via the equation-of-motion (EOM) or response CC approach [15]. This means that we represent the excited-state wave functions  $|\Psi_\mu\rangle$  as  $|\Psi_\mu\rangle = R_\mu \exp(T)|\Phi_0\rangle$ , where in the CCSD case  $R_\mu$  is a sum of the reference ( $R_0$ ), 1p-1h ( $R_1$ ), and 2p-2h ( $R_2$ ) components,  $R_\mu = R_0 + R_1 + R_2$ , and  $T = T_1 + T_2$ . In the excited-state CR-CC(2,3) and CR-CC(2,4) methods, the results of the EOM CCSD calculations are corrected for the effects of  $T_3$  and  $R_3$  [CR-CC(2,3)] or  $T_3$ ,  $T_4$ ,  $R_3$ , and  $R_4$  [CR-CC(2,4)] through the suitably designed energy corrections [14]. Again, the main idea is to avoid the large costs of high-order CC schemes for excited states.

Table I gives the energies of the ground-state ( $0^+$ ) and the first  $2^+$  and  $4^+$  excited states as functions of the shell gap in the various levels of approximation. Figure 1(a) compares the CR-CC(2,3), CISDTQ, and full CI results. We see that the CR-CC(2,3) and CISDTQ approximations track each other very closely for all shell gaps. This includes the region of small shell gaps and overlaps  $S_0$ , where the reference determinant  $|\Phi_0\rangle$  is a poor representation of the ground state. This shows that one can use

TABLE I. Energies (in MeV) of  $^{56}\text{Ni}$  as functions of the shell-gap shift  $\Delta G$  (also in MeV), relative to the reference energy  $\langle\Phi_0|H|\Phi_0\rangle$ .  $S_0$  is defined as  $|\langle\Phi_0|\Psi_0^{\text{Full-CI}}\rangle|$ .

$\Delta G$		-2	-1	0	1	2
State	$S_0$	0.022	0.332	0.825	0.917	0.949
$0^+$	CCSD	-3.218	-2.048	-1.509	-1.202	-1.002
	CR-CC(2,3)	-4.355	-2.437	-1.686	-1.298	-1.060
	CR-CC(2,4)	-4.253	-2.415	-1.679	-1.295	-1.059
	CISD	-2.148	-1.652	-1.327	-1.104	-0.943
	CISDT	-2.706	-1.946	-1.488	-1.199	-1.004
	CISDTQ	-4.013	-2.548	-1.758	-1.334	-1.079
	Full CI	-10.198	-3.868	-1.909	-1.370	-1.091
$2^+$	T2D	0.260	0.158	0.113	0.088	0.072
	CCSD	-2.440	-0.065	1.595	2.983	4.241
	CR-CC(2,3)	-2.695	-0.218	1.496	2.915	4.192
	CR-CC(2,4)	-2.700	-0.222	1.493	2.913	4.190
	CISD	0.864	2.000	3.093	4.162	5.215
	CISDT	-1.227	0.359	1.771	3.066	4.283
	CISDTQ	-2.426	-0.335	1.378	2.833	4.137
$4^+$	Full CI	-9.728	-3.054	0.689	2.594	4.027
	REL	1.309	1.178	1.114	1.080	1.060
	CCSD	-1.373	0.910	2.551	3.942	5.211
	CR-CC(2,3)	-1.667	0.720	2.420	3.848	5.141
	CR-CC(2,4)	-1.626	0.736	2.428	3.852	5.144
	CISD	1.554	2.743	3.884	4.994	6.082
	CISDT	-0.271	1.301	2.713	4.017	5.248
$4^+$	CISDTQ	-1.465	0.606	2.308	3.769	5.087
	Full CI	-8.700	-1.974	1.778	3.581	4.999
	REL	1.333	1.215	1.152	1.115	1.090

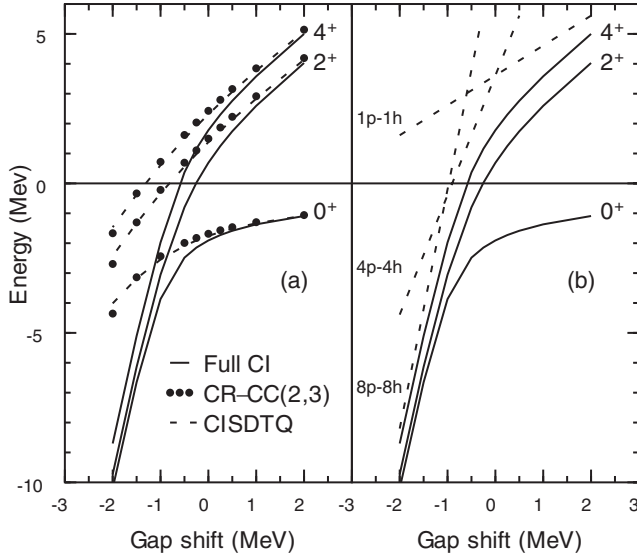


FIG. 1. (a) The full CI, CISDTQ, and CR-CC(2,3) energies of  $^{56}\text{Ni}$  as functions of the shell-gap shift  $\Delta G$ . (b) Comparison of full CI energies with the trends expected for the 1p-1h, 4p-4h, and 8p-8h configurations as functions of  $\Delta G$ .

inexpensive CC methods, such as CR-CC(2,3), to obtain the results that in the shell-model description are equivalent to the CISDTQ calculations. Thus, if CISDTQ is accurate enough for the nuclear properties of interest, one can save an enormous amount of computer effort by performing CC calculations of the CR-CC(2,3) type. In our case, the CISDTQ and CR-CC(2,3) approaches are reasonable up to about  $\Delta G \approx 0$ , but for  $\Delta G < 0$ , where the shell gap and overlap  $S_0$  substantially decrease, the CISDTQ and CR-CC(2,3) energies diverge from the full CI results. We can understand this by analyzing Fig. 1(b), where we compare the full CI energies of the  $0^+$ ,  $2^+$ , and  $4^+$  states, plotted as functions of  $\Delta G$ , with the trends expected for various  $np$ - $nh$  components. The energy curves of the  $2^+$  and  $4^+$  states approach the slope characterizing the 1p-1h components as the gap is increased. This perfectly correlates with the very good performance of the basic CCSD and CR-CC(2,3) approximations in the  $\Delta G > 0$  region. The experience of quantum chemistry is that these kinds of CC approximations describe excited states dominated by 1p-1h components almost exactly. We observe the same behavior here. At  $\Delta G = 0$ , the excited states corresponding to the predominantly 4p-4h configurations start at an excitation energy of 5.0 MeV [1]. The 4p-4h line in Fig. 1(b) is drawn to go through 5 MeV at  $\Delta G = 0$ , which is the bandhead energy of the deformed band [1]. By comparing the slopes of energy curves with the slopes of the  $np$ - $nh$  lines in Fig. 1(b), we can see that 4p-4h correlations gain in importance in the  $\Delta G \approx 0$  region, but higher-than-4p-4h correlations remain unimportant. This explains why the CISDTQ and CR-CC(2,3) approximations, which can accurately describe excitations up to 4p-4h, work well in the  $\Delta G > 0$  region. However, as the gap is

decreased further and we enter the  $\Delta G < 0$  region, the energies of all states rapidly go down, approaching the slope of the 8p-8h components. For  $\Delta G = -2$  MeV, the 8p-8h correlations are so strong that they become the dominant part of the ground-state band, which shows a strong rotational character. The CC methods used in this study, which provide an accurate description of up to 4p-4h correlations but neglect  $T_n$  clusters with  $n > 4$  and disconnected product terms involving  $T_3$  and  $T_4$ , are not applicable when the 8p-8h correlations become dominant. The same applies to CISDTQ. It should be noted, however, that independent of the shell gap, CCSD is more accurate than the corresponding CISD approximation in spite of the fact that both approaches rely on up to 2p-2h excitations. CR-CC(2,3) is always more accurate than CISDT, although both approaches use up to 3p-3h excitations.

The performance of the CC methods used in this study, which rely on the spherical reference state  $|\Phi_0\rangle$ , correlates with the overlap  $S_0$  between  $|\Phi_0\rangle$  and the full CI ground state  $|\Psi_0^{\text{Full-CI}}\rangle$ . Small overlaps  $S_0$  that accompany small shell gaps enhance the magnitude of higher-than-4p-4h correlations and this causes problems for basic CC approximations, such as CR-CC(2,3), and truncated CI methods, including CISDTQ. Table I indicates that we obtain excellent results with CR-CC(2,3) when  $S_0 \geq 0.9$ . In this study, we have access to full CI wave functions, so that we know the exact  $S_0$ . However, one usually does not know the exact value of  $S_0$ . For this reason, it is useful to propose a diagnostic, based on truncated CC calculations, which could tell us when the CC results are trustworthy. For the CC methods relying on CCSD, one can propose such diagnostic by realizing that the  $T_2$  clusters increase when the shell gap and  $S_0$  decrease. Thus, we define the “ $T_2$  diagnostic” (T2D), using  $T_2$  clusters obtained in the CCSD calculations, as  $(\langle\Phi_0|T_2^\dagger T_2|\Phi_0\rangle/n_0)^{1/2}$ . We divide the connected (i.e., size extensive) quantity  $\langle\Phi_0|T_2^\dagger T_2|\Phi_0\rangle$ , which represents the  $T_2$  cluster contributions to the wave function, by  $n_0$  to make T2D independent of the system size. As shown in Table I, T2D correlates with  $S_0$ , providing us with a simple way of assessing the applicability of single-reference CC methods. According to Table I, the CR-CC(2,3) approach is accurate when T2D is 0.1 or smaller. We also give in Table I the “Reduced Excitation Level” (REL) [16], which enables one to characterize the  $np$ - $nh$  nature of the excited state using the reference 1p-1h and 2p-2h components of the excitation operator  $R_\mu$  resulting from the EOM CCSD calculations. The CR-CC(2,3) and CR-CC(2,4) methods describe excited states well if REL does not exceed 2.0, provided that  $T_2$  clusters are not too large. In our case, REL does not exceed 1.333. Thus, the main reason for the inaccuracies in excited-state results in the region of smaller shell gaps is a small  $S_0$ , reflected in the larger values of T2D. This can be understood, since the EOM CC methods are equivalent to response CC approaches [15]; i.e., inaccuracy in the ground state results propagates into excited states.

TABLE II.  $C_3$  excitation and  $T_3$  cluster contributions to the ground-state energy for different values of  $\Delta G$  (all in MeV).

$\Delta G$	-2	-1	0	1	2
CISDT-CISD	-0.559	-0.294	-0.162	-0.095	-0.060
CR-CC(2,3)-CCSD	-1.138	-0.388	-0.177	-0.096	-0.059

Finally, we explain why the CR-CC(2,3) approach is as accurate as the more expensive CISDTQ method. We begin with the ground-state results. In this case, the 1p-1h components of the wave function vanish due to symmetry, so that the  $np$ - $nh$  excitation operators  $C_n$  defining the CI expansion of the ground state (assuming the intermediate normalization condition  $\langle \Phi_0 | \Psi_0 \rangle = 1$ ) can be expressed in terms of the  $np$ - $nh$  cluster components  $T_n$  as follows:  $C_1 = T_1 = 0$ ,  $C_2 = T_2$ ,  $C_3 = T_3$ , and  $C_4 = T_4 + (T_2)^2/2$ . The CR-CC(2,3) approach provides an accurate description of  $T_1$ ,  $T_2$ , and  $T_3$  contributions. An accurate representation of the 3p-3h contributions by CR-CC(2,3) is verified in Table II, which shows that the  $C_3$  contributions, extracted from CI by forming the difference of the CISDT and CISD energies, and the corresponding  $T_3$  contributions, obtained by subtracting the CCSD energy from the CR-CC(2,3) energy, are indeed similar (they begin to differ at  $\Delta G = -2$  MeV, but this is a strongly correlated region where one cannot cleanly extract the  $C_n$  and  $T_n$  contributions). The above relationships between  $C_n$  and  $T_n$  imply that the CISDTQ and CR-CC(2,3) results will agree as long as  $T_4$  cluster contributions are small. As shown in Table I, the CR-CC(2,4) and CR-CC(2,3) energies are virtually identical, showing that  $T_4$  contributions are indeed negligible. In other words, the presence of the disconnected 4p-4h clusters  $(T_2)^2/2$  in CC calculations is the main reason for the observed similarity between the CR-CC(2,3) and CISDTQ results. Product terms of this type represent the leading 4p-4h excitations. To have them in CI, one has to go all the way up to the CISDTQ approximation. The CC methods bring such terms at lower levels, such as CCSD. A similar analysis can be carried out for excited states. For states of different symmetry than the ground state, such as  $2^+$  and  $4^+$ , one can write the following:  $C_1 = R_1$ ,  $C_2 = R_2$ ,  $C_3 = R_3 + R_1 T_2$ , and  $C_4 = R_4 + R_2 T_2 + R_1 T_3$ . Again, the similarity of CR-CC(2,3) and CR-CC(2,4) energies implies that  $R_4$  is small. Thus, we can express the  $C_n$  components with  $n = 1-4$  using the  $R_1$ ,  $R_2$ , and  $R_3$  components of  $R_\mu$  and the  $T_1$ ,  $T_2$ , and  $T_3$  components of  $T$ , which are accurately described by CR-CC(2,3).

In summary, we compared the CC and CI results for  $^{56}\text{Ni}$  obtained in the  $pf$  shell basis. By varying the gap between the  $f_{7/2}$  orbit and the  $f_{5/2}$ ,  $p_{3/2}$ ,  $p_{1/2}$  orbits, we tested a few practical CC approximations, such as CR-CC(2,3), that can be applied to systems with dozens or hundreds of correlated fermions and hundreds of single-particle basis states, as a function of the weight of the reference determinant in the wave function and the strength of the higher-order

correlation effects. We showed that independent of the shell gap, the results of CR-CC(2,3) calculations are close to those obtained with the more demanding CI calculations truncated at 4p-4h configurations. The practical CC methods, such as CR-CC(2,3), provide accurate results as long as the overlap between the reference determinant and the exact wave function is greater than 0.9 or as long as the values of the proposed  $T_2$  diagnostic, T2D, are 0.1 or less. We may be able to extend the applicability of inexpensive CC methods of the CR-CC(2,3) type to heavier nuclei with a less closed-shell character by refining the reference-state determinant, so that the T2D values do not exceed 0.1 over a wider range of shell gaps. This may be possible if we replace the closed-shell reference state [e.g., the  $(f_{7/2}^{16})$  configuration used in this work] by the deformed state resulting from mean-field calculations or if we turn to CC approaches that use multideterminantal reference states.

Supported by the National Science Foundation and the U.S. Department of Energy. We thank Morten Hjorth-Jensen for help with the matrix elements of the GXPF1A Hamiltonian. We also thank Morten Hjorth-Jensen, David Dean, and Thomas Papenbrock for discussions.

- 
- [1] M. Horoi *et al.*, Phys. Rev. C **73**, 061305(R) (2006).
  - [2] F. Coester, Nucl. Phys. **7**, 421 (1958); F. Coester and H. Kümmel, Nucl. Phys. **17**, 477 (1960).
  - [3] J. Čížek, J. Chem. Phys. **45**, 4256 (1966); Adv. Chem. Phys. **14**, 35 (1969).
  - [4] H. Kümmel, K. H. Lüthmann, and J. G. Zabolitzky, Phys. Rep. **36**, 1 (1978); R. F. Bishop, in *Lecture Notes in Physics*, edited by J. Navarro and A. Polls (Springer, Berlin, 1998), Vol. 510, p. 1.
  - [5] J. Paldus and X. Li, Adv. Chem. Phys. **110**, 1 (1999).
  - [6] P. Piecuch *et al.*, Int. Rev. Phys. Chem. **21**, 527 (2002).
  - [7] J. H. Heisenberg and B. Mihaila, Phys. Rev. C **59**, 1440 (1999); B. Mihaila and J. H. Heisenberg, Phys. Rev. C **61**, 054309 (2000).
  - [8] K. Kowalski *et al.*, Phys. Rev. Lett. **92**, 132501 (2004); M. Włoch *et al.*, Phys. Rev. Lett. **94**, 212501 (2005); J. R. Gour *et al.*, Phys. Rev. C **74**, 024310 (2006).
  - [9] C. J. Cramer *et al.*, J. Phys. Chem. A **110**, 1991 (2006).
  - [10] M. Honma *et al.*, Eur. Phys. J. A **25**, Suppl. 1, 499 (2005).
  - [11] M. Hjorth-Jensen, T. T. S. Kuo, and E. Osnes, Phys. Rep. **261**, 125 (1995).
  - [12] M. Honma *et al.*, Phys. Rev. C **65**, 061301(R) (2002); Phys. Rev. C **69**, 034335 (2004).
  - [13] G. D. Purvis and R. J. Bartlett, J. Chem. Phys. **76**, 1910 (1982).
  - [14] P. Piecuch *et al.*, Chem. Phys. Lett. **418**, 467 (2006); M. Włoch *et al.*, Mol. Phys. **104**, 2149 (2006).
  - [15] K. Emrich, Nucl. Phys. **A351**, 379 (1981); H. J. Monkhorst, Int. J. Quantum Chem.: Quantum Chem. Symp. **11**, 421 (1977); J. F. Stanton and R. J. Bartlett, J. Chem. Phys. **98**, 7029 (1993).
  - [16] M. Włoch *et al.*, J. Chem. Phys. **122**, 214107 (2005).